Comparative Study of Nanostructured TiO₂ and SLA Surface Modifications for Titanium Implants: Surface Morphology and *in vitro* Evaluation

Elisa Marchezini[a]* ⓘ, Tatiane Cristine Silva de Almeida[a], Fernanda de Paula Oliveira[a],

Juliano Douglas Silva Albergaria[b], Santunu Ghosh[a], Mariana Andrade Boense Tavares[a],

Ramon Resende Leite[a], Gerluza Aparecida Borges Silva[b], Maximiliano D. Martins[a] ⓘ

[a]Centro de Desenvolvimento da Tecnologia Nuclear, Belo Horizonte, MG, Brasil.
[b]Universidade Federal de Minas Gerais, Instituto de Ciências Biológicas, Departamento de Morfologia,
Belo Horizonte, MG, Brasil.

Our work presents a comparative study of morphological characteristics and the osteogenic potential of MC3T3-E1 cells on different modified surfaces of titanium: nanostructured TiO₂ with 20 and 100 nm nanotube diameter, and sandblasting and acid etching, commercially known as SLA. Nanostructured TiO₂ surface was prepared by anodizing of titanium plates, while SLA surface was provided by commercial supplier. Surfaces were characterized by SEM, EDS, AFM, and water contact angle measurements. In order to evaluate cell response, *in vitro* tests of MTT, alkaline phosphatase and staining with alizarin red were performed. From the results of *in vitro* tests, 100 nm nanotubular surface showed lower levels of cell mineralization, differentiation and adhesion. In general, 20 nm TiO₂ nanotubular and SLA surfaces promoted similar response from osteoblasts. As a result, 20 nm nanotubular surface proved to be a possible alternative to SLA surface with potential for use in oral implantology market.

Keywords: *Titanium, Anodic Oxidation, Surface Modification, Osseointegrated Implants, Biomaterials.*

1. Introduction

Titanium and its alloys are currently the most preferred materials for the manufacture of dental implants[1-3]. The intrinsic physical and chemical features of titanium, such as excellent biocompatibility[2,4], good fatigue[5], high corrosion resistance[6], relatively low modulus of elasticity[7,8] and machinability[9], are advantageous for the manufacture of dental implant devices. In addition to these characteristics, modifications are commonly made on implant surface to stimulate osteogenic differentiation and extracellular matrix deposition, when compared to unmodified surfaces. These modifications increase the bone-implant contact area, the anchorage and the osseointegration process, which results the increase of implants duration and decrease of recovery time after surgery[10,11]. Examples of surface modifications applied to titanium implants are: sand blasting, acid etching, plasma spraying, electrochemical micro-arc oxidation and anodic oxidation (anodizing)[12,13].

One of the most commercially used surface modification techniques is SLA-treated surface that consists of the combination of two sequential processes: large-grit sand particles and acid etching[12]. A retrospective study assessed a decade of outcomes of titanium implants with an SLA surface in a large group of partially edentulous patients. This analysis resulted in a survival rate of 98.8% and a success rate of 97.0%. In addition, the prevalence of peri-implantitis in these patients was low with 1.8%[14]. In addition, numerous studies on the SLA surface containing *in vitro* assays evaluating characteristics such as cell viability, mineralization, adhesion, among others, point to satisfactory results for the SLA surface[15-18].

Despite the good results obtained from the SLA surface, the researchers are constantly looking for alternatives to improve the performance of dental implants and investigating other forms of surface modification. The anodizing process has been shown to be a possible alternative for surface modification due to its easy implementation and low cost, in addition to improving the osseointegration process of dental implants[2,19-22]. It is an electrochemical method which uses an electrolyte with a low concentration of fluoride ions ($0.1 – 1\%w$) that produces an oxide layer (TiO_2) in the form of vertically aligned nanotubes through the passage of electrical current[23-25].

Although anodizing time, electrolyte temperature and composition influence the oxide layer characteristics, but the applied voltage is one of the most important parameters used during the anodizing process of Ti[26,27]. As demonstrated by Bauer *et al*.[28], as the applied tension increases, there is a linear relationship with the increase in the pore diameter. Recent studies have shown that the adhesion and function of osteoblasts cultured in a layer of TiO₂ nanotubes manufactured by anodizing can be improved compared to their non-anodized

counterparts[29,30]. However, the *in vitro* effects of TiO_2 nanotubes of different diameters have controversial results.

Some researchers related the best biological performance to the presence of the nanotubular titania layer with an internal nanotube diameter of less than 30 nm. Park *et al*.[31] reported that the average diameters between 15 and 30 nm are more favorable to stimulate the formation of focal points through integrin assembly, which induces assembly of actin filaments and signaling to the nucleus. Nanotubes larger than 70 nm diameter do not support focal contact formation and cell signaling, affecting adhesion and proliferation of mouse mesenchymal stem cells, limiting cell activity and causing cell death. In another study Park *et al*.[32] observed that, both osteoclast differentiation and osteoblast proliferation were improved for nanotube diameters between 15 and 20 nm. They also observed that the formation of philopodia is considerably enhanced in samples with nanotube diameter of 15 nm in comparison with those of 100 nm. Similarly, Bauer *et al*.[33] reported the behavior of mesenchymal stem cells in layers of ZrO_2 and TiO_2 nanotubes produced by anodizing and the comparison of their behavior on smooth surfaces. For both surfaces, adhesion and maximum cell activity were obtained when nanotubes in the range of 15 to 30 nm in diameter were present.

On the other hand, different studies have demonstrated good biological performance for nanotubular titanium surfaces with a nanotube diameter around 100 nm. Malec *et al*.[30] evaluated the influence of nanotubular TiO_2 with diameters of 80 and 108 nm on the cell response in osteoblastic lineage of progenitors derived from human adipose tissue. The results indicated that the nanostructured TiO_2 is a safe and non-toxic biomaterial.

Thus, the aim of this work was to compare the behavior of osteoblasts on TiO_2 nanotubular surfaces of two different diameters (20 and 100 nm) with SLA surface (sand blasted and acid etched), through *in vitro* tests.

2. Materials and Methods

Disc-shaped titanium plates were used as substrates (9.5 mm of diameter and 2 mm thick), with two types of surfaces: nanotubular and SLA (sandblasted and acid etched). SLA samples - titanium discs sandblasted with high purity aluminum oxide - Al_2O_3 (> 99%) and treated with HNO_3 + HF - were supplied by PecLab Ltda., a dental implant manufacturer. Anodized samples were prepared in 0.5 wt% HF + 1 mol/L H_3PO_4 electrolyte, at 20 °C, for 90 min, under voltages of 5 and 25 V, as detailed in our previous work[34]. After surface preparation, compositional, morphological, and topographic properties of Ti modified sample surfaces were characterized by scanning electron microscopy (SEM-FEG SIGMA-VP, Carl Zeiss, SEM/FIB Quanta FEG 3D FEI and SEM/FEG Quanta 200 FEI) and energy Dispersive X-ray Spectroscopy (EDS-XFlash 410M, Brucker), 10 samples of each group and Atomic Force Microscopy (AFM, NTREGRA, NT-MDT), 3 samples of each group.

The contact angle measurements of the nanotubular TiO_2 and SLA surfaces were performed using the static drop method, in which a 3 µL drop of distilled water were deposited on the sample surface with a microsyringe. The goniometer (Pixelink DGD Inst DI) of the Laboratory of Polymer and Composite Engineering of the Department of Metallurgical and Materials Engineering of UFMG was used. The contact angle values were reported from the average of five more measurements, taken in different sections of the sample, which were obtained using the Digidrop software, which uses an algorithm that determines the average value of contact angle in relation to measurements.

To evaluate the cellular response as a function of the diameter of TiO_2 nanotubes produced on Ti surfaces, two nanotube sizes were used: 20 and 100 nm. In addition, SLA samples were also used for comparison, as this is an implant surface well established on the market. Sample sterilization was performed by gamma irradiation at a dose of 15 kGy, using a Cobalt-60 gamma source (model IR-214, type GB-127, Nordion Inc., Canada) located in the Gamma Irradiation Laboratory of the Centro de Desenvolvimento da Tecnologia Nuclear (CDTN).

Cells of MC3T3-E1 subclone 14 lineage, immortalized pre-osteoblasts from newborn mice calvaria were used in this study, marketed by the company ATCC (Manassas, Virginia; www.atcc.org). For cultivation, these cells were removed from the liquid nitrogen stock and then thawed in a 37 °C water bath. The cell suspension was transferred to a sterile plastic bottle containing basal culture medium composed of Alpha Minimum Essential Medium (α-MEM; Gibco™) supplemented with 10% Fetal Bovine Serum (FBS; Gibco™) and streptomycin antibiotics (100 µg/mL) / penicillin (500 U/mL; Invitrogen™). Then, the flask containing the cell suspension was centrifuged for 7 min at 1400 RPM. Subsequently, the pellet containing the cells was resuspended in 10 mL of fresh basal medium and the cell suspension was added to the sterile cell culture bottle (Sarstedt, 75 cm²) and incubated in an oven at 37 °C, in an atmosphere of 5% CO_2.

To perform the *in vitro* assays, three samples from each group were placed in a 48-well plate and then MC3T3-E1 pre-osteoblast cells were seeded at $3x10^4$ density per well. After plating, they were incubated in an oven at 37 °C in a humid atmosphere with 5% CO_2. As a control group, all procedures performed in each *in vitro* assay were performed in empty wells, without any sample.

The cytotoxicity of biomaterials was assessed using the 3-(4,5-dimethylthiazol-2-yl)-2,5-diphenyl-2H-tetrazolium bromide (MTT) assay (Life Technologies). The test was carried out after periods of 3 and 7 days. After the proposed times, the culture medium was then removed and a solution containing 130 µL of basal medium, composed of α-MEM and 100 µL of MTT (5 mg/mL)/well was added. After 2 h, formazan crystals were visualized under a light microscope and then dissolved in 130 µL of 10% SDS in 0.01 mol/L HCl (Sigma-Aldrich®). In all steps of the above description, the culture plates were incubated at 37 °C, 5% CO_2. After 18 hours, 100 µL of the centrifuged solution was transferred, in triplicate, to a 96-well plate and the optical density was measured in a spectrophotometer (Biotek, uQuant) at a wavelength of 595 nm.

For the evaluation of cell differentiation, the activity of alkaline phosphatase was evaluated using the kit of bromo-4-chloro-3-indolyl phosphate (BCIP), nitro-blue tetrazolium salt (NBT). The groups were evaluated at the end of 7 and

Comparative Study of Nanostructured TiO$_2$ and SLA Surface Modifications for Titanium Implants: Surface Morphology and *in vitro* Evaluation

3

14 days. In the chosen periods for analysis, the culture medium was discarded and cells were washed with PBS. After discarding the PBS, cells were incubated with 200 µL/well of NBT/BCIP solution, in the proportion of 1:1:8 in PBS for 2 h, at 37 °C and 5% CO$_2$. After confirming the presence of blue precipitates under an optical microscope, 210 µL/well of sodium dodecyl sulfate (SDS) was added, a detergent that smooths the cells, 10% + HCl without removing the incubated NBT/BCIP solution. To promote the solubilization of the precipitates, the plates were incubated for 18 h (overnight). After this period, 100 µL of each well were transferred, in triplicate, to a 96-well plate and the optical density was measured in a spectrophotometer (Biotek, uQuant) at a wavelength of 595 nm.

For the analysis of the potential of mineral deposition by staining with alizarin red, the cells received supplemented α-MEM medium and added osteogenic solution (2.165 mg/mL ß-glycerolphosphate + ascorbic acid) (Sigma–Aldrich®). The plates were kept in an incubator at 5% CO$_2$ by 14 and 21 days. At the end of the experiment, the supernatant was collected and cells were washed with sterile 1x PBS having pH 7.4. Then, cells were fixed with 70% ethanol for 1 h in the refrigerator. After removing the fixative, the wells were washed with distilled water and 200 µL of the solution of the alizarin red dye (Sigma–Aldrich®), at a concentration of 40 mmol/L, pH 4.2, maintained under stirring for 20 min. Subsequently, the dye was removed and the wells were washed again in distilled water. Then, 200 µL of 10% cetylpyridinium chloride were added to the wells, which were kept under stirring for 30 min. After the shaking period, 100 µL of each well was transferred, in triplicate, to a new flat-bottom culture plate and the optical density was measured on the spectrophotometer (Biotek, uQuant) at a wavelength of 550 nm.

The cell morphology was investigated using the scanning electron microscopy (SEM). To perform the test, cells on the samples surfaces and kept in a CO$_2$ incubator for a period of 3, 7 and 14 days. Each of the wells containing the samples was washed twice with 150 µL of phosphate buffer at a concentration of 0.1 mol/L. Afterwards, 150 µL of 2.5% glutaraldehyde fixing solution in phosphate buffer at a concentration of 0.1 mol/L were added to each well. The specimens were kept in contact with the fixative solution for 24 h at 4 °C. After this period, the fixative solution was removed and discarded, and 150 µL of 0.1 mol/L phosphate buffer was added. Then the samples were fixed in osmium tetroxide, dehydrated and dried in a critical CO$_2$ point.

Cell adhesion was assessed by direct fluorescence using phalloidin (Life Technologies) conjugated to green fluorescent dye FITC (Invitrogen™), and DAPI - 4',6-diamidino-2-phenylindole dihydrochloride (Life Technologies) for nuclear DNA staining. To perform this, at first cells were washed twice with PBS, pH 7.4, fixed in a 3.7% formaldehyde solution in PBS for 10 min at room temperature and again washed twice with PBS. Then 0.1% triton X-100 in PBS was added for 3 to 5 min and cells were again washed twice with PBS. Then, 10 µL of the stock solution was diluted in 200 µL of PBS for each sample to be stained. This solution was then placed in the wells by 20 min at room temperature. After that time, cells washing was performed twice with PBS. Subsequently, the cells were incubated for 30 min with 100 µL of a 10 µg/mL solution of fluorescent streptavidin solution. The plates were incubated for 15 min at room temperature and then washed with PBS. The images were made using an Olympus BX-50 microscope. Cell counting was performed by determining the number of nuclei stained with DAPI of 7 images of each group, using the Quantikov software[35]. The statistical data analysis was performed using the GraphPad Prism software version 5.0 (https://www.graphpad.com/). The data were represented as mean ± standard deviation and compared statistically using one-way ANOVA analysis of variance followed by the Tukey posttest, with p <0.05.

3. Results and Discussion

The SEM images of SLA sample is shown on the Figure 1. The SLA surface presents microscopic roughness with protrusions produced by blasting with Al$_2$O$_3$ distributed equally throughout the sample. Figure 2 shows SEM images of anodized samples with an applied voltage of 5 and 25 V, with a magnification of 200,000x. The image analysis shows that the anodized surfaces exhibit nanotubular morphology for the two values of applied tension, with nanotubes with rounded ends. Anodizing performed under 5 and 25 V voltage produced nanotubes with an average diameter of 21.0 ± 4.7 nm and 103.4 ± 20.5 nm, respectively. For the sake of simplicity, nanotubes with approximately 20 and 100 nm of
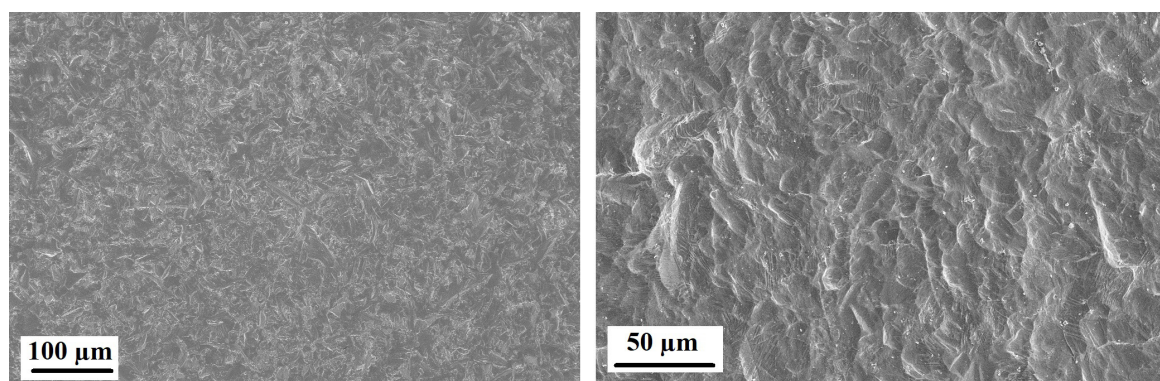

100 µm   **50 µm**

Figure 1. SEM images of SLA sample. Magnification: 300x (left) and 1000x (right).

diameter will be indicated as $TiO_2/20$ and $TiO_2/100$ respectively throughout the manuscript.
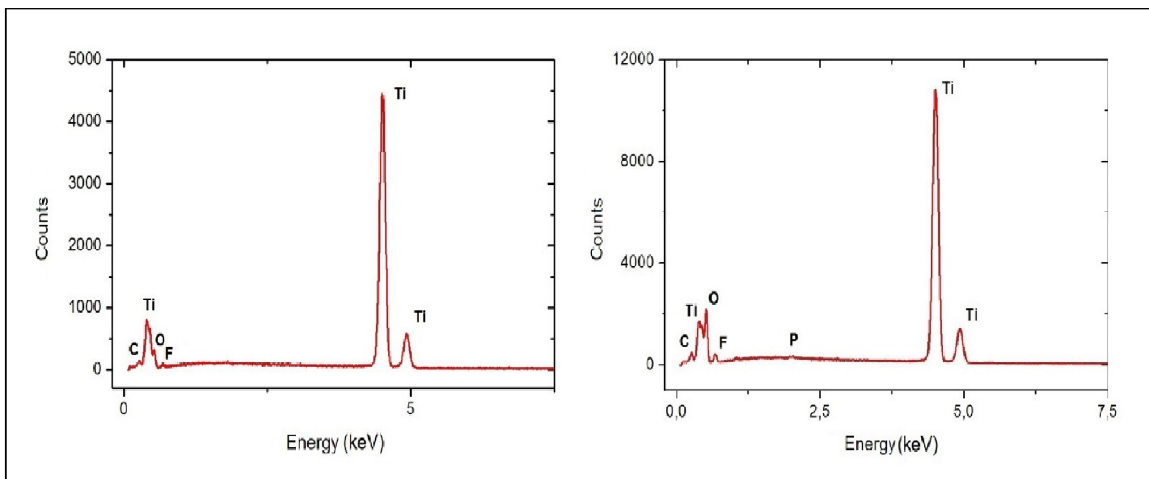
Figure 3 shows the results of the analysis carried out by EDS on $TiO_2/20$ and $TiO_2/100$ samples. EDS analysis indicates the presence of titanium (Ti) and oxygen (O), from the substrate and the oxide on the surface, fluorine (F), remaining from the electrolyte used in the anodization and carbon (C), on both surfaces. In addition, a small amount of phosphorus, another elementary electrolyte species, was also found, but only on the $TiO_2/100$ sample. According to Jain *et al.*[36], the amount of P incorporated in the surface increases with the increase of the applied voltage, which may explain the fact that P is not detected on the $TiO_2/20$ sample, as it is deposited under a very low voltage. Previous studies[37,38] revealed that the presence of P on the surface of an implant can help to accelerate the osseointegration process, as it is a component of the main phosphate compound (hydroxyapatite $[Ca_{10}(PO_4)_6(OH)_2]$) present in bone and dental tissues. The analysis of EDS spectrum on the SLA sample (Figure 4) showed the presence

of Ti, originated from the substrate, as well as a small peak of O appears due to the thin layer of titanium oxide formed on the surface of the substrate and also a peak of Al appears due to the AL_2O_3 blasting.

The presence of Al is considered a contaminant on the sample surface and this element should be completely removed after the acid treatment to which the sample was subjected[39]. Frequently, the presence of Al is observed on the surfaces of implants obtained by blasting with Al_2O_3, and these impurities may interfere the osseointegration process[40]. However, the presence of Al on the SLA surface evaluated in the present study, apparently did not interfere with osteoblast viability. This result agrees with the study reported by Sader *et al.*[39], in which they have tested two types of titanium surfaces sandblasted with alumina. They observed that the differentiation and mineralization of osteoblasts on those surfaces didn't result any negative effect on the development of osteoblasts due to the residual alumina present on the surface.
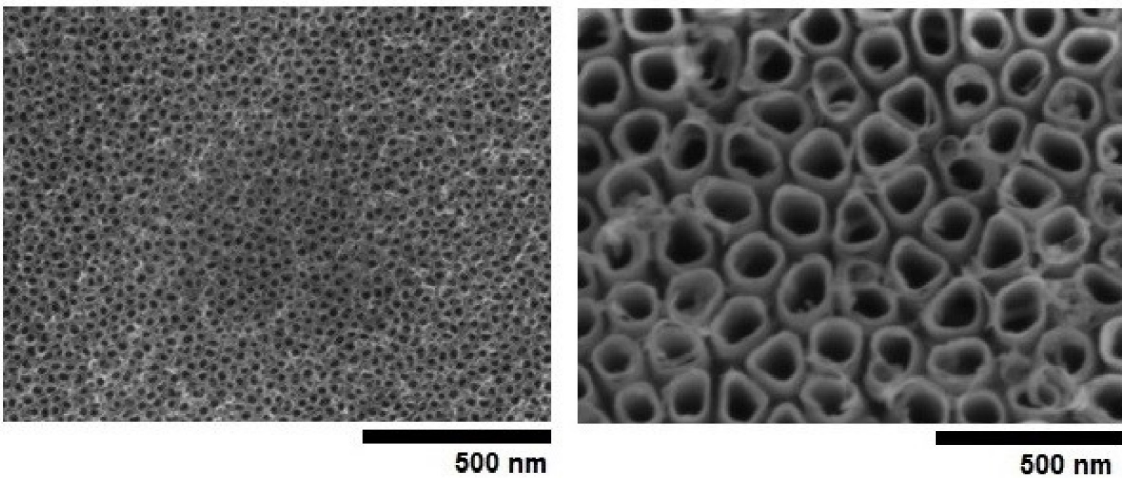
Figure 2. SEM images after preparation of the TiO_2 nanotubular layer on titanium as a function of the anodizing voltage: 5 V (left) and 25 V (right). Magnification: 200,000 x.

Figure 3. EDS spectra of $TiO_2/20$ (left) and $TiO_2/100$ (right) samples.

Comparative Study of Nanostructured TiO₂ and SLA Surface Modifications for Titanium Implants: Surface Morphology and *in vitro* Evaluation

5

Table 1 presents the measured roughness values obtained from AFM measurement (R_a – average roughness; R_y – peak to peak; R_z – ten-point height; R_q – root mean square; R_{sk} – surface skewness; R_{ka} – coefficient of kurtosis) for the three surfaces in the area of 100×100 μm². The roughness parameters are dependent on the sampled area and their values increase with increasing scale. Due to the Al_2O_3 blasting, the SLA surface had the highest Ra value, equal to (673.6 ± 0.2) nm, followed by the two nanotubular surfaces, with Ra $= (349.7 \pm 0.3)$ nm for TiO₂/100 and Ra $= (206.2 \pm 0.1)$ nm for TiO₂/20 sample, shown on the Table 1. The results of the existing roughness values in the literature for nanotubular surfaces are contradictory. Jain *et al*.[36] reported that the roughness of these surfaces is greater for the larger diameter of the nanotubes and our present study follows the similar trend. However, Brammer *et al*.[41] compared the roughness of nanotubular surfaces with diameters of 30, 50 and 100 nm and found that the mean roughness values without a significant difference between them. The influence of surface roughness on the behavior of osteoblasts will be discussed later in this manuscript.

Table 2 presents the average value of the contact angle of each surface, and its respective population standard deviation. The contact angle of a drop of water on a given surface is measured in order to assess its wettability. In general, hydrophilic surfaces are more favorable to osseointegration because in contact with blood and biological fluids they promote protein adsorption and improve cell adhesion. On the other hand, hydrophobic surfaces can partially denature proteins, modifying their structure and making cell binding sites less accessible, which results in less cell adhesion[42,43].

Previous studies exhibit that the SLA surface has wettability values greater than 90°, thus being a hydrophobic surface, with contact angles from 120° to 138°[40,44]. However, in this study, the wettability measurement performed on the SLA surface showed a value of 91.3°, demonstrating that the SLA surface is less hydrophobic. The other two tested surfaces in this study showed that they are hydrophilic surfaces, that is, they have wettability values much lower than 90° and much lower than that of SLA surface. For example, Brammer *et al*[41]. presented contact angle values for TiO₂ nanotubular surfaces of 30 and 100 nm as 11° and 4°, respectively. Comparing with the values obtained in the present work, the values are close: 18° for the TiO₂/20 and 1.6° for the TiO₂/100 surface. In another study, Kummer *et al*.[43] measured the contact angle for nanotubular TIO₂ surfaces with nanotube diameter of 20 and 80 nm. The measured values were approximately 8° to 30°, which means these surfaces are hydrophilic. In contrast, Aguirre *et al*.[21] measured the contact angle on nanotubular TiO₂ surfaces obtained with acetic acid with different sources of F⁻ ions, with anodizing voltages of 10 and 15 V, with and without heat treatment. These surfaces presented varied contact angles, from 6.8° to 113.7°, showing no well-defined correlation between the diameter of TiO₂ nanotubes and the hydrophilicity of the surface, suggesting that other factors should influence the wettability of surfaces, such as anodizing conditions.

Figure 5 illustrates the evolution of cell viability, over the time of 3 and 7 days, for each evaluated surface. The MTT assay showed that cell viability for 3 days and 7 days had no statistical difference in the cell proportion evaluated on the three surfaces: SLA, TiO₂/20 and TiO₂/100 surfaces. The results suggest that these proposed Ti modified surfaces did not interfere with cell viability. Evaluating the results of this test, an increase in viability was observed from 3 to 7 days on the three surfaces and, although in 3 days the SLA surface showed a tendency to be more viable than the other surfaces, there was no statistical difference among any of them. Considering that the SLA surface is proven to be viable and non-toxic[45] and that the three surfaces presented values
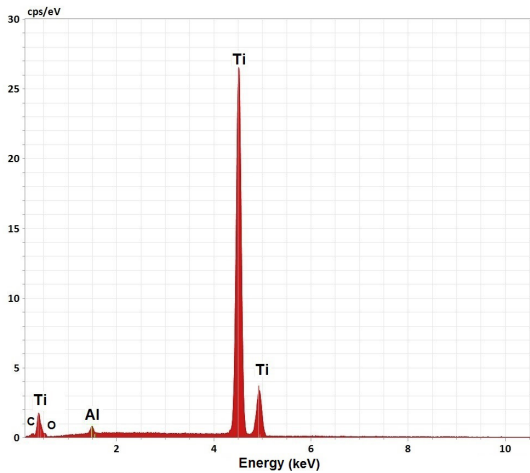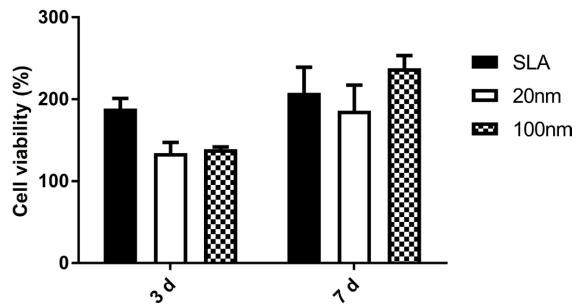
Figure 4. EDS spectrum of SLA sample.

Figure 5. Viability (%) of MC3T3-E1 cells obtained by MTT assay after 3 and 7 days of cultivation on SLA, TiO₂/20 and TiO₂/100 surfaces. One-way ANOVA test followed by Tukey test. Data expressed as mean ± SEM. *vs SLA ($p < 0.05$) and #vs 20 nm ($p < 0.05$).

Table 1. Roughness parameters of TiO₂/20, TiO₂/100 and SLA samples performed with a 100×100 μm² scan.

Sample	R_a (nm)	R_y (nm)	R_z (nm)	R_q (nm)	R_{sk}	R_{ka}
SLA	673.6	7129.0	3491.7	850.8	0.062	0.169
TiO₂/20	206.2	2077.9	1043.7	260.1	0.133	0.031
TiO₂/100	349.7	3187.3	1590.5	455.3	0.250	0.342

Table 2. Average values of contact angle for SLA, TiO$_2$/20 and TiO$_2$/100 samples.

Surface	Contact angle (degrees)
SLA	91.3 ± 0.5
TiO$_2$/20	18.3 ± 1.1
TiO$_2$/100	1.6 ± 0.8

close to viability, it can be understood that the nanotubular surface is as viable as the SLA.

At 7 days, no statistical difference was observed in the values presented for the production of alkaline phosphatase in the three groups evaluated (Figure 6). The SLA surface showed higher alkaline phosphatase production compared to both anodized surfaces at 14 days. Previous studies have demonstrated the influence of surface roughness on alkaline phosphatase activity, which is higher on surfaces with higher values of roughness parameter, as surfaces with this characteristic promote the adhesion of osteogenic cells to the surface[40,46]. At 14 days, a high cell differentiation value is observed for the SLA surface, which is also the roughest surface of the three. Evaluating the nanotubular surfaces in the same period, both presented very different levels of differentiation, with this value on the TiO$_2$/100 surface slightly higher than on the TiO$_2$/20 surface, also following the respective roughness values.

The bone matrix mineralization degree was assessed by the red alizarin assay, after 14 and 21 days of culture (Figure 7). In the period of 14 days, mineralization showed a slight tendency to increase the amount of mineral in contact with the SLA and TiO$_2$/20 surfaces comparing to the TiO$_2$/100 surface. When the results of the percentage of mineralized matrix in the period of 21 days are evaluated, a trend is observed in the increase of the percentage of mineralization for the TiO$_2$/20, when compared to the other evaluated surfaces. The results of the test with alizarin red staining exhibit an increase in the mineralization of the nanotubular surfaces from 14 to 21 days, while the SLA surface remains practically stable in both periods. Huang *et al.*[47] observed the same behavior of nanotubular and SLA surfaces in their study.

Cell adhesion and morphology were also investigated by fluorescence microscopy, which allows for better identification of the cytoskeleton, through its labeling using fluorescent dye FITC - phalloidin (green) and the labeling of the nuclei, using DAPI (blue). Figure 8 shows the images obtained by fluorescence microscopy of pre-osteoblast cells cultured for 3, 7 and 14 days on the three different surfaces (SLA, TiO$_2$/20 and TiO$_2$/100). It is observed that on the TiO$_2$/100 surface (3 days) cells grew randomly in a smaller amount, when compared to the SLA and TiO$_2$/20 surfaces at the same time. It can also be observed that some cells formed pseudopods on the 3 surfaces. The fluorescence markings of the cytoskeleton and nucleus revealed a great confluence of pre-osteoblast cells cultured on the SLA and TiO$_2$/20 surfaces in 7 and 14 days, with formation of cellular multilayers, thus suggesting a greater cell adhesion, the same type of behavior was not observed on the TiO$_2$/100 surface. Figure 9 shows the graph obtained from the quantification of nuclei stained with DAPI. This quantification was only
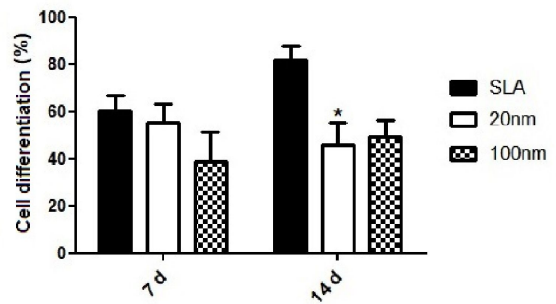
Figure 6. Differentiation (%) of pre-osteoblast cells obtained by alkaline phosphatase assay after 7 and 14 days of culture on SLA, TiO$_2$/20 and TiO$_2$/100 surfaces. One way ANOVA test followed by Tukey test. Data expressed as mean ± EPM. *vs SLA (p <0.05) and #vs 20 nm (p <0.05).
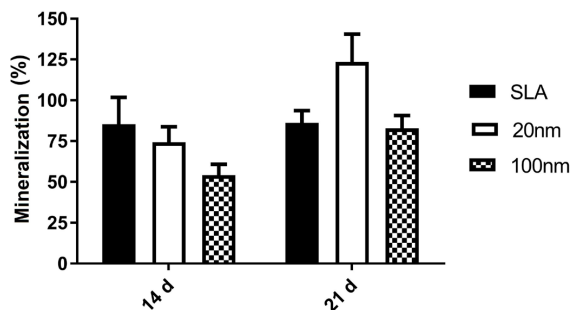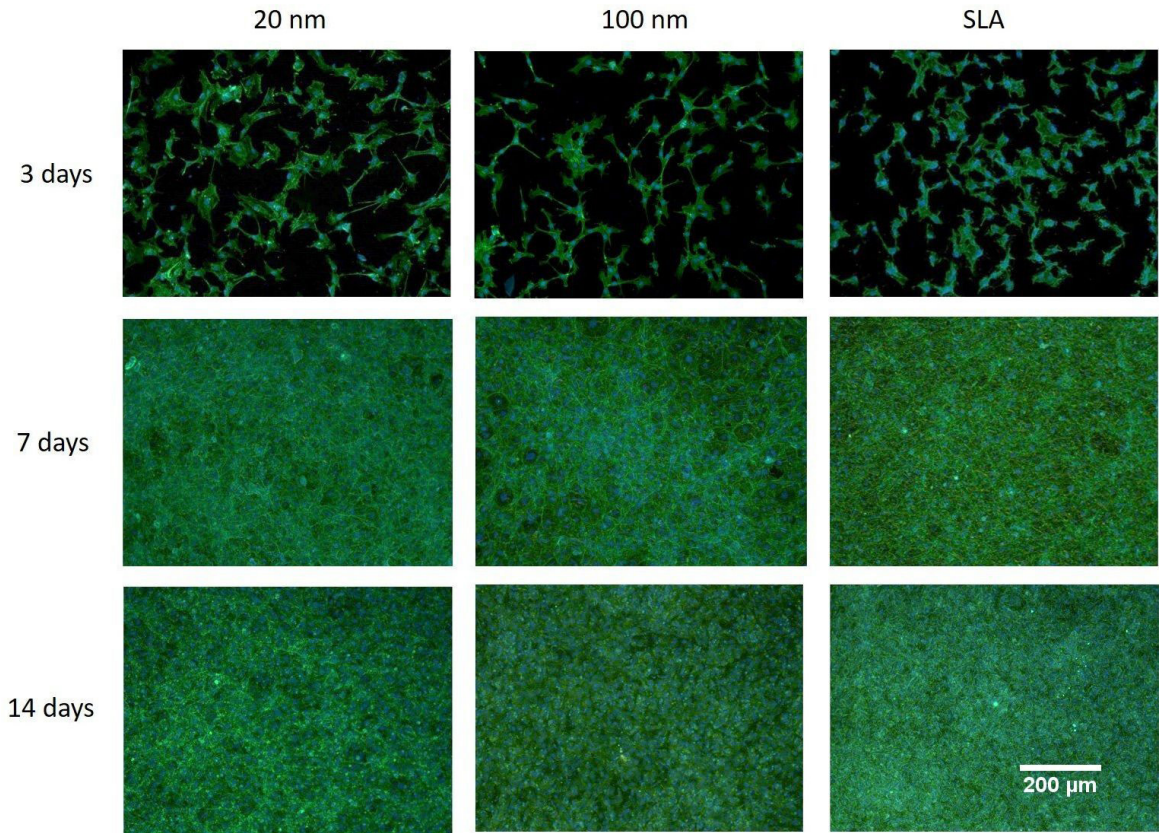

Figure 7. Analysis of osteoblast mineralization grown for 14 and 21 days on SLA, TiO$_2$/20 and TiO$_2$/100 surfaces. One-way ANOVA test followed by Tukey test. Data expressed as mean ± EPM. *vs SLA (p <0.05) and #vs 20 nm (p <0.05).

possible for the periods of 3 and 7 days, since in the period of 14 days the large number of cells on the 3 surfaces made it impossible to separate the nuclei for the counting.

The cell quantification obtained showed a large increase in the number of cells in contact with all surfaces tested from 3 to 7 days, demonstrating osteoblast adhesion on the three surfaces. In addition, a greater number of cells could be observed on the TiO$_2$/20 surface after 3 days, compared to the TiO$_2$/100 surface, and this difference was remained in the cell culture time of 7 days. In this same period, there is also a significant difference between the SLA and TiO$_2$/100 surfaces. Relating the cell adhesion results to the contact angle values obtained in the present study for the three surfaces, a direct relationship between these two parameters was not observed. On contrary, previous studies reported that the increase in adhesion is directly related to the increase in hydrophilicity[42]. In both periods in which the adhered cells were quantified, 3 and 7 days, from the three surfaces, TiO$_2$/100 was the one with the lowest number of adhered cells. For the two hydrophilic surfaces such as SLA and TiO$_2$/20, TiO$_2$/20 showed more adhered cells than the less hydrophilic (SLA).

Figure 10 shows the SEM images of adhered cells to titanium modified surfaces after 3, 7 and 14 days of culture, which made it possible to qualitatively assess the

Comparative Study of Nanostructured TiO$_2$ and SLA Surface Modifications for Titanium Implants: Surface Morphology and *in vitro* Evaluation

7

Figure 8. Morphology and adhesion of MC3T3-E1 cells cultured for 3, 7 and 14 days on three different surfaces (SLA, TiO$_2$/20 and TiO$_2$/100), observed by fluorescence microscopy.
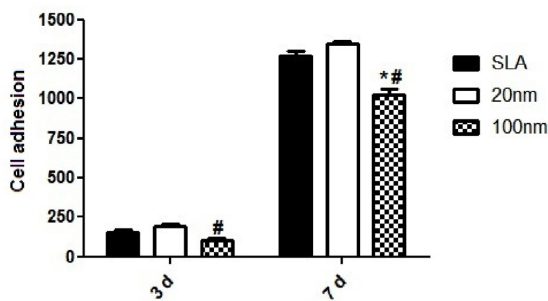

Figure 9. Quantification of the nuclei of MC3T3-E1 cells grown for 3 and 7 days on three different surfaces (SLA, TiO$_2$/20 and TiO$_2$/100). One-way ANOVA test followed by Tukey test. Data expressed as mean ± EPM. *vs SLA ($p < 0.05$) and #vs 20 nm ($p < 0.05$).

morphological aspect of the cells. Cells have a flat and polygonal morphology with several cytoplasmic extensions, similar types of observations were found in previous studies[47,48]. After 3 days of culture, pre-osteoblasts proliferate on SLA, TiO$_2$/20 and TiO$_2$/100 surfaces. Cells on the SLA surface showed rounded morphology with few cytoplasmic extensions, characteristic of undifferentiated cells. Apart from that, cells on both nanotubular surfaces showed a characteristic morphological stage of cell differentiation, flattened and starry cell form with communicating cytoplasmic extensions.

However, there is still a small difference between them: cells on TiO$_2$/100 surface have a morphology slightly more elongated and less spread out than cells on TiO$_2$/20 surface. Such morphological characteristics of the cells observed in the SEM images obtained shown in Figure 10, and it can also be observed in the fluorescence images, obtained by an optical microscope (Figure 8).

At both times of 7 and 14 days, SLA surface exhibits a large number of cells, covering a large part of the sample surface, where they had a flattened appearance, starry with pronounced and evident filamentous cytoplasmic extensions (philopodia), initiating connections between cells. The same was observed on the TiO$_2$/20 surface, but with a smaller number of cells in 7 days. Cells in contact with TiO$_2$/100 surface were smaller, less numerous, more elongated, less scattered and low formation of philopodia morphology, compared to the other two tested surfaces (TiO$_2$/20 and SLA), which suggests that this surface promotes certain adhesion difficulties, less proliferation and less cellular activity in cells.

Relating the results obtained by SEM with the levels of mineralization, obtained by the alizarin red test, at 14 days, it is possible to see a concordance between both, where greater formation of philopodia (higher mineralization level) by the cells is observed on the SLA and on the TiO$_2$/20 surfaces. The TiO$_2$/100 surface, on the other hand, was clearly the one that least developed a mineralized matrix, observing a much lower amount of philopodia compared to the
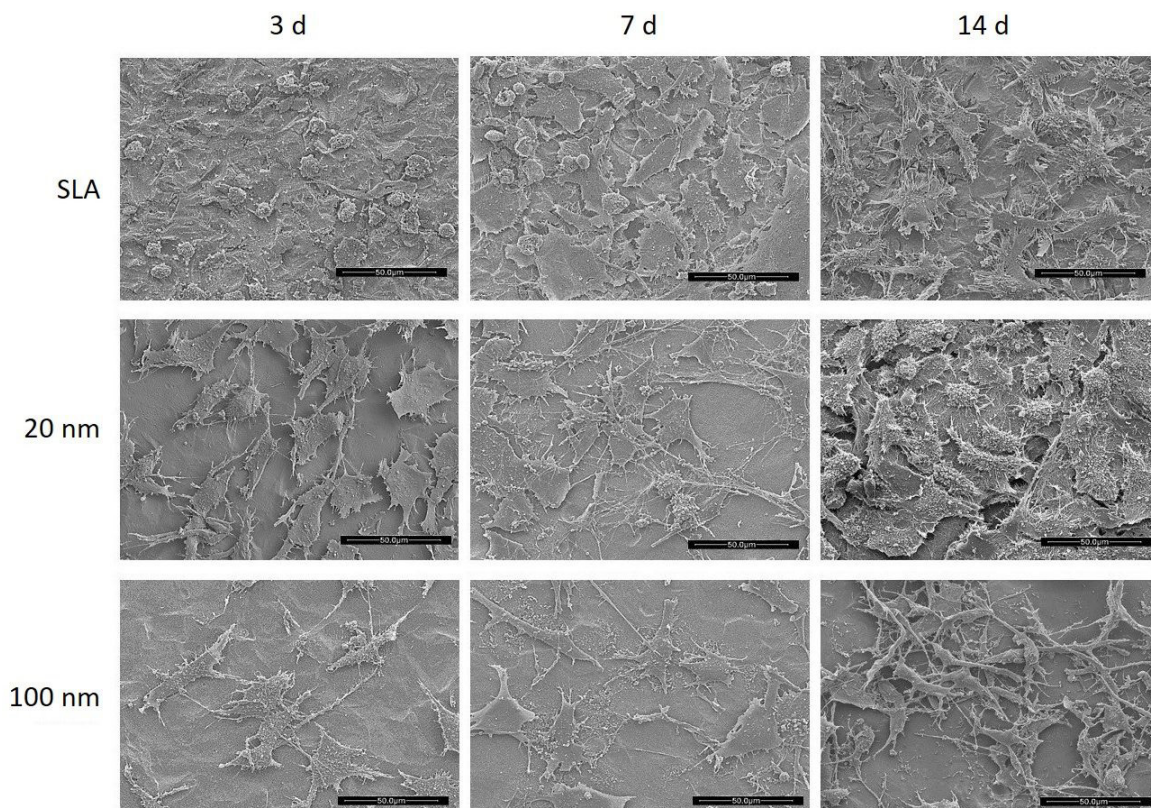
Figure 10. Morphology of MC3T3-E1 cells cultured for 3, 7 and 14 days on three different surfaces (SLA, $TiO_2/20$ and $TiO_2/100$), observed by scanning electron microscopy.

$TiO_2/20$ surface. The same types of trends were observed in the study of Park *et al*.[31]. They reported that, in an evaluation of the behavior of osteoblasts on different TiO_2 nanotubular surfaces (from 15 to 100 nm) and on a smooth Ti surface, the mineralization is greater for the smaller the diameter of the nanotubes. Their study also reported that, nanotubes with diameters greater than 50 nm prevent cell adhesion and dissemination, and 100 nm nanotubes almost completely prevent integrin grouping and formation of focal adhesion complexes, resulting in reduced proliferation, differentiation and cell mineralization. In the present work, in the SEM image in Figure 10, it was observed that although both cells have flattened morphology, on the $TiO_2/20$ surface the cell has a greater amount of philopodia than on the $TiO_2/100$ surface, as also occurred in the study of Park *et al*.[32]

4. Conclusions

The main goal of this study was to explore the osteogenic behavior of nanotubular TiO_2 surface modification as compared to a standard and well-stablished surface modification applied to titanium-based osseous implant (the SLA surface). The results of *in vitro* assays performed on the nanotubular TiO_2 surfaces with average nanotube diameter of 20 nm, 100 nm and SLA surface modification showed no cytotoxicity of the three surfaces, moreover, the two nanotubular surfaces showed cellular viability similar to that of the SLA surface. Our results suggest that TiO_2 nanotubular surface modification

with average nanotube diameter of 20 nm is a promising route for surface modification of titanium-based dental implants aiming to increase the cellular functions that lead to osseointegration.

5. Acknowledgments

6. References

1. Özcan M, Hämmerle C. Titanium as a reconstruction and implant material in dentistry: advantages and pitfalls. Materials (Basel). 2012;5:1528-45.

2. Kulkarni M, Mazare A, Gongadze E, Perutkova Š, Kralj-Iglič V, Milošev I, et al. Titanium nanostructures for biomedical applications. Nanotechnology. 2015;26:062002.

3. Nicholson JW. Titanium alloys for dental implants: a review. Prosthesis. 2020;2:100-16.

4. Louarn G, Salou L, Hoornaert A, Layrolle P. Nanostructured surface coatings for titanium alloy implants. J Mater Res. 2019;34:1892-9.

5. Velasco-Ortega E, Flichy-Fernández A, Punset M, Jiménez-Guerra A, Manero JM, Gil J. Fracture and fatigue of titanium narrow dental implants: new trends in order to improve the mechanical response. Materials (Basel, Switzerland). 2019;12:3728.

6. Souza JCM, Apaza-Bedoya K, Benfatti CAM, Silva FS, Henriques B. A comprehensive review on the corrosion pathways

Comparative Study of Nanostructured TiO₂ and SLA Surface Modifications for Titanium Implants: Surface Morphology and *in vitro* Evaluation

9

of titanium dental implants and their biological adverse effects. Metals (Basel). 2020;10:1272.

7. Brizuela A, Herrero-Climent M, Rios-Carrasco E, Rios-Santos JV, Pérez RA, Manero JM, et al. Influence of the elastic modulus on the osseointegration of dental implants. Materials (Basel, Switzerland). 2019;12:980.

8. Pérez-Pevida E, Brizuela-Velasco A, Chávarri-Prado D, Jiménez-Garrudo A, Sánchez-Lasheras F, Solaberrieta-Méndez E, et al. Biomechanical consequences of the elastic properties of dental implant alloys on the supporting bone: finite element analysis. BioMed Res Int. 2016;2016:1850401-1850401.

9. Elias CN, Fernandes DJ, Souza FM, Monteiro ES, Biasi RS. Mechanical and clinical properties of titanium and titanium-based alloys (Ti G2, Ti G4 cold worked nanostructured and Ti G5) for biomedical applications. J Mater Res Techn. 2019;8:1060-9.

10. Kligman S, Ren Z, Chung CH, Perillo MA, Chang YC, Koo H, et al. The impact of dental implant surface modifications on osseointegration and biofilm formation. J Clin Med. 2021;10:1641.

11. Wang LN, Jin M, Zheng Y, Guan Y, Lu X, Luo JL. Nanotubular surface modification of metallic implants via electrochemical anodization technique. Int J Nanomedicine. 2014;9:4421-35.

12. Jemat A, Ghazali MJ, Razali M, Otsuka Y. Surface modifications and their effects on titanium dental implants. BioMed Res Int. 2015;2015:791725-791725.

13. Ma T, Ge X, Zhang Y, Lin Y. Effect of titanium surface modifications of dental implants on rapid osseointegration. In: Sasaki K, Suzuki O, Takahashi N, eds. Interface oral health science. Singapore: Springer; 2016. p. 247-56.

14. Buser D, Janner FSM, Wittneben JG, Brägger U, Ramseier CA, Salvi GE. 10-Year survival and success rates of 511 titanium implants with a sandblasted and acid-etched surface: a retrospective study in 303 partially edentulous patients. Clin Implant Dent Relat Res. 2012;14:839-51.

15. Zhang J, Liu J, Wang C, Chen F, Wang X, Lin K. A comparative study of the osteogenic performance between the hierarchical micro/submicro-textured 3D-printed Ti6Al4V surface and the SLA surface. Bioact Mater. 2020;5:9-16.

16. Gu YX, Du J, Si MS, Mo JJ, Qiao SC, Lai HC. The roles of PI3K/Akt signaling pathway in regulating MC3T3-E1 preosteoblast proliferation and differentiation on SLA and SLActive titanium surfaces. J Biomed Mater Res A. 2012;101(3):748-54.

17. Li LJ, Kim SN, Cho SA. Comparison of alkaline phosphatase activity of MC3T3-E1 cells cultured on different Ti surfaces: modified sandblasted with large grit and acid-etched (MSLA), laser-treated, and laser and acid-treated Ti surfaces. J Adv Prosthodont. 2016;8:235-40.

18. Li H, Huang J, Wang Y, Chen Z, Li X, Wei Q, et al. Nanoscale modification of titanium implants improves behaviors of bone mesenchymal stem cells and osteogenesis *in vivo*. Oxid Med Cell Longev. 2022;2022:13.

19. Traini T, Murmura G, Sinjari B, Perfetti G, Scarano A, D'Arcangelo C, et al. The surface anodization of titanium dental implants improves blood clot formation followed by osseointegration. Coatings. 2018;8:252.

20. Minagar S, Berndt CC, Wang J, Ivanova E, Wen C. A review of the application of anodization for the fabrication of nanotubes on metal implant surfaces. Acta Biomater. 2012;8:2875-88.

21. Aguirre R, Echeverry-Rendón M, Quintero D, Castaño JG, Harmsen MC, Robledo S, et al. Formation of nanotubular TiO₂ structures with varied surface characteristics for biomaterial applications. J Biomed Mater Res A. 2018;106:1341-54.

22. İzmir M, Ercan B. Anodization of titanium alloys for orthopedic applications. Front Chem Sci Eng. 2019;13:28-45.

23. Roy P, Berger S, Schmuki P. TiO₂ nanotubes: synthesis and applications. Angew Chem Int Ed. 2011;50:2904-39.

24. Susin C, Finger Stadler A, Musskopf ML, Rabelo MS, Ramos UD, Fiorini T. Safety and efficacy of a novel, gradually anodized dental implant surface: a study in yucatan mini pigs. Clin Implant Dent Relat Res. 2019;21:44-54.

25. Nyamukamba P, Okoh O, Mungondori H, Taziwa R, Zinya S. Synthetic methods for titanium dioxide nanoparticles: a review. In: Yang D, eds. Titanium dioxide – Material for a sustainable environment. London: IntechOpen; 2018. p. 151-75.

26. Ocampo RA, Echeverría FE. Effect of the anodization parameters on TiO₂ nanotubes characteristics produced in aqueous electrolytes with CMC. Appl Surf Sci. 2019;469:994-1006.

27. Kulkarni M, Mazare A, Schmuki P, Igli P. Influence of anodization parameters on morphology of TiO₂ nanostructured surfaces. Advanced Materials Letters. 2016;7:23-8.

28. Bauer S, Kleber S, Schmuki P. TiO₂ nanotubes: tailoring the geometry in H₃PO₄/HF electrolytes. Electrochem Commun. 2006;8:1321-5.

29. Li G, Zhao Q, Tang HP, Li G, Chi T. Fabrication, characterization and biocompatibility of TiO₂ nanotubes via anodization of Ti6Al7Nb. Compos Interfaces. 2016;23:223-30.

30. Malec K, Góralska L, Hubalewska-Mazgaj M, Głowacz P, Jarosz M, Brzewski P, et al. Effects of nanoporous anodic titanium oxide on human adipose derived stem cells. Int J Nanomedicine. 2016;11:5349-60.

31. Park J, Bauer S, von der Mark K, Schmuki P. Nanosize and vitality: TiO₂ nanotube diameter directs cell fate. Nano Lett. 2007;7:1686-91.

32. Park J, Bauer S, Schlegel KA, Neukam FW, von der Mark K, Schmuki P. TiO₂ nanotube surfaces: 15 nm - an optimal length scale of surface topography for cell adhesion and differentiation. Small. 2009;5:666-71.

33. Bauer S, Park J, Faltenbacher J, Berger S, von der Mark K, Schmuki P. Size selective behavior of mesenchymal stem cells on ZrO₂ and TiO₂ nanotube arrays. Integr Biol. 2009;1:525-32.

34. Marchezini E, Oliveira FP, Lopes R, Almeida TCS, Gastelois PL, Martins MD. Controlling morphological parameters of a nanotubular TiO₂ coating layer prepared by anodic oxidation. Mater Res Express. 2020

35. Pinto LCM. Quantikov - Um analisador microestrutural para o ambiente WindowsTM [thesis]. São Paulo: Instituto de Pesquisas Energéticas e Nucleares, Universidade de São Paulo; 1996.

36. Jain S, Williamson RS, Janorkar AV, Griggs JA, Roach MD. Osteoblast response to nanostructured and phosphorus-enhanced titanium anodization surfaces. J Biomater Appl. 2019;34:419-30.

37. Kar A, Raja KS, Misra M. Electrodeposition of hydroxyapatite onto nanotubular TiO₂ for implant applications. Surf Coat Tech. 2006;201:3723-31.

38. Kunze J, Müller L, Macak J, Greil P, Schmuki P, Müller F. Time-dependent growth of biomimetic apatite on anodic TiO2 nanotubes. Electrochim Acta. 2008;53:6995-7003.

39. Sader MS, Balduino A, Soares GA, Borojevic R. Effect of three distinct treatments of titanium surface on osteoblast attachment, proliferation, and differentiation. Clin Oral Implants Res. 2005;16:667-75.

40. Le Guehennec L, Lopez-Heredia MA, Enkel B, Weiss P, Amouriq Y, Layrolle P. Osteoblastic cell behaviour on different titanium implant surfaces. Acta Biomater. 2008;4:535-43.

41. Brammer KS, Oh S, Frandsen CJ, Jin S. Biomaterials and biotechnology schemes utilizing TiO₂ nanotube arrays. In: Pignatello R, ed. Biomaterials science and engineering. London: IntechOpen; 2011. p. 193-210.

42. Gittens RA, Scheideler L, Rupp F, Hyzy SL, Geis-Gerstorfer J, Schwartz Z, et al. A review on the wettability of dental implant

surfaces ii: biological and clinical aspects. Acta Biomater. 2014;10:2907-18.

43. Kummer KM, Taylor EN, Durmas NG, Tarquinio KM, Ercan B, Webster TJ. Effects of different sterilization techniques and varying anodized TiO$_2$ nanotube dimensions on bacteria growth. J Biomed Mater Res B Appl Biomater. 2013;101B:677-88.

44. Rupp F, Scheideler L, Eichler M, Geis-Gerstorfer J. Wetting behavior of dental implants. Int J Oral Maxillofac Implants. 2011;26:1256-66.

45. Lagonegro P, Trevisi G, Nasi L, Parisi L, Manfredi E, Lumetti S, et al. Osteoblasts preferentially adhere to peaks on micro-structured titanium. Dent Mater J. 2018;37:278-85.

46. Carmo LC Fo, Martins APP, Bielemann AM, Possebon APR, Faot F. Simplified micrometric surface characterization of different implant surfaces available on the brazilian market. Braz J Oral Sci. 2018;17:e18371.

47. Huang J, Zhang X, Yan W, Chen Z, Shuai X, Wang A, Wang Y. Nanotubular topography enhances the bioactivity of titanium implants. Nanomedicine. 2017;13(6):1913-23. https://doi.org/10.1016/j.nano.2017.03.017.

48. Bello DG, Fouillen A, Badia A, Nanci A. A nanoporous titanium surface promotes the maturation of focal adhesions and formation of filopodia with distinctive nanoscale protrusions by osteogenic cells. Acta Biomater. 2017;60:339-49.